Structural style of the Makran Tertiary accretionary complex in SE-Iran

12

J.-P. Burg, A. Dolati, D. Bernoulli, and J. Smit

Introduction

Theories on the internal dynamics of wedges largely refer to the concept of critical wedge (e.g. Chapple 1978; Davis et al. 1983). The concept considers that the mechanics of thrust-belts is analogous to pushing sand, i.e. material that follows the Mohr–Coulomb failure criterion, in front of a moving bulldozer. How much of these assumptions is applicable to natural wedges requires direct geological studies, with emphasis on structures because their geometry constrains rheology and the general behaviour of a compressional system. As discussed by Platt et al. (1988), theories on the internal dynamics of wedges need to be confronted with observation of spatial and time variations, but tests are lacking because most active examples are submarine (Barbados, Costa Rica, Nankai, Eastern Mediterranean) whilst ancient wedges have been affected by later collision tectonics (e.g. Shongpan–Ghanzi, East Anatolia). Their large-scale characteristics are interpreted from seismic profiles (e.g. Westbrook et al. 1988; Fruehn et al. 2002) and many sand-box experiments have simulated their bulk behaviour and growth (e.g. Westbrook et al. 1988; Schott and Koyi 2001; Kukowski et al. 2002; Konstantinovskaya and Malavieille 2011).

We report new structural observations from the Makran Accretionary Wedge (MAW), in Iran, a region that has been little studied for many years. Our intention was to study the geology and structures of this denuded area to constrain the structural behaviour of accretionary wedges. The "regional" objective was to understand the role of Makran among the Tethys subduction-collision zones.

Makran, geologically defined, is one of the largest accretionary wedges on Earth. Located in SE Iran and South Pakistan, it extends ca. 1,000 km from the Strait of Hormuz in the west to near Karachi in the east (Fig. 12.1). The width of the wedge is 300–350 km from the offshore front of deformation to the depressions of Jaz Murian in Iran and Mashkel in Pakistan (Fig. 12.1). More than half of the wedge is exposed onland. The active, frontal part is submarine, in the Sea of Oman. Three features make the MAW especially interesting: (1) Outcrop conditions are extremely good, allowing direct and continuous geological observation over areas larger than in any other exposed accretionary wedge; (2) Folded and imbricated turbidite successions occur farther inland than younger slope-facies mudstones and coastal deposits; therefore, different deformation styles and stages can be distinguished and (3) The Makran has not been deformed by continental collision tectonics, hence exposes pre-collision deformation features and wedge fabric that may still be recognized in collision orogens.

Basic fieldwork included the re-evaluation of the stratigraphy and standard structural geology. Detailed sections with systematic sampling make the skeleton of a new geological map covering the central part of the on-shore MAW (Dolati 2010). This map takes advantage of high-resolution multi-spectral Landsat7 ETM+ and MrSID images on areas mapped in less details to correlate the stratigraphic and structural profiles. We expect that this contribution will offer a framework for further structural analysis and modelling of wedges and enable ongoing stratigraphic and geochronological analyses to be focused efficiently.

J.-P. Burg (✉) · A. Dolati · D. Bernoulli · J. Smit
ETH and University Zurich, Sonneggstrasse 5,
CH-8092 Zürich, Switzerland
e-mail: jean-pierre.burg@erdw.ethz.ch

A. Dolati
Geological Survey Iran, Meraj Street, Azadi Square,
13185-1494 Tehran, Iran
e-mail: Asghar.dolati@gmail.com

D. Bernoulli
Geology Institute, University of Basel, Bernoullistrasse 32,
CH-4056 Basel, Switzerland
e-mail: Daniel.Bernoulli@unibas.ch
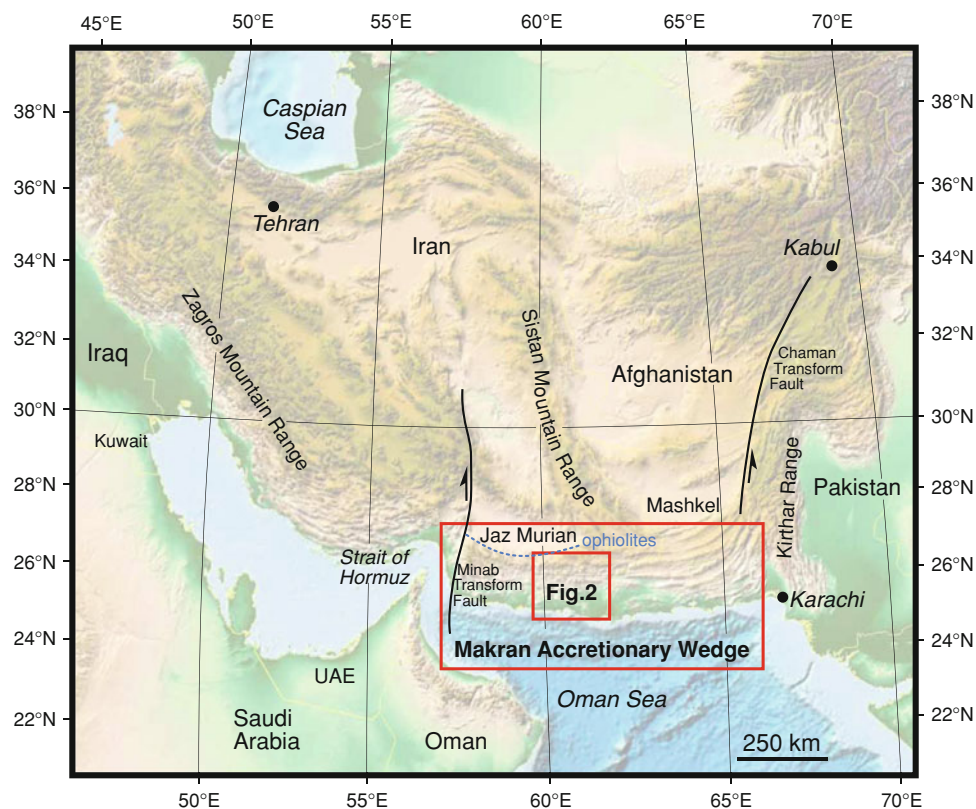
Tectonic Context

The Makran is an uplifted, Eocene–Recent accretionary complex that extends over ca. 1,000 km between the dextral Minab Transform Fault through the Strait of Hormuz, to the west, and the sinistral Chaman Transform Fault, along the Kirthar Range to the east (Fig. 12.1). The ophiolite-bearing imbricate zone (so-called "coloured mélange" of McCall 1983) separating the Jaz-Murian Basin, to the north, from the MAW sensu stricto to the south (Fig 12.1) is accepted as a segment of the Tethys orogenic system (e.g. Şengör et al. 1988; Ricou 1994). The MAW is a key orogenic feature produced from the convergence between the Arabian and Eurasian plates taking place since at least the Late Cretaceous (e.g. De Jong 1982; Dercourt et al. 1993). The MAW is now associated with the ongoing subduction of the oceanic lithosphere flooring the Gulf of Oman at a present-day rate of about 2 cm.a^{-1} in a roughly N–S direction, beneath the Iran and Afghan Blocks (McQuarrie et al. 2003; Bayer et al. 2006; Vigny et al. 2006; Masson et al. 2007). This subduction is responsible for the andesitic volcanic arc traced 300–500 km to the north of the coast so that the Jaz-Murian and Mashkel depressions (Fig. 12.1) are interpreted to be fore-arc basins (Farhoudi and Karig 1977; McCall

1997); however, the age of the Makran volcanic arcs (Bazman in Iran and Chagai Hills in Pakistan) suggests that subduction started already earlier in the Late Cretaceous (e.g. Arthurton et al. 1982; Berberian et al. 1982; McCall and Kidd 1982). Shortening and abundant sediment supply led the low-taper wedge to grow seawards by frontal accretion and underplating of trench fill sediments (Platt et al. 1985, 1988; Kopp et al. 2000). The modern MAW developed since the Early–Middle Miocene, leading to a typical thrust-and-fold belt with forward propagation of thrusting, sediment underplating at the front and subsequent thickening and uplift of the accretionary complex (Kukkonen and Clauser 1994; Kopp et al. 2000; Schlüter et al. 2002; Ellouz-Zimmermann et al. 2007a, b). Frontal accretion and continued sediment underthrusting take place along a northward-stepping detachment (Harms et al. 1984; Fruehn et al. 1997). Earthquake hypocentres and offshore seismic reflection and refraction show that the subducting oceanic plate dips <3° to the north (e.g. White and Klitgord 1976; White 1982; Kopp et al. 2000), apparently reaching a depth of 30 km below the Jaz Murian depression (e.g. Byrne et al. 1992; Kopp et al. 2000). Seismic tomography images also a shallow-dipping slab below the Eurasian continent (Bijwaard et al. 1998; Hafkenscheid et al. 2006).
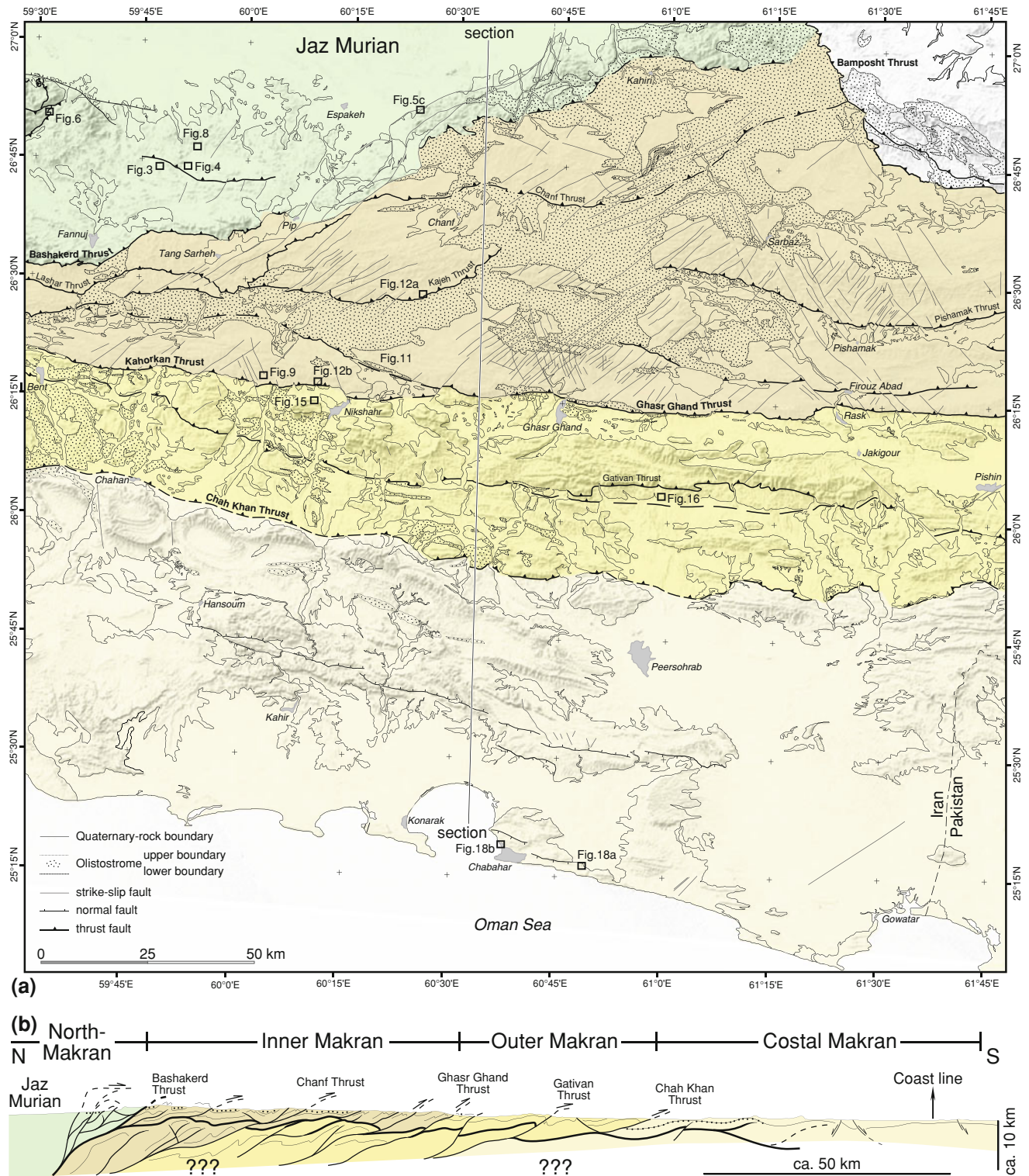
Fig. 12.2 a Simplified map of Central Makran in Iran. *Green* North Makran of mostly Cretaceous rocks; *Brown* Inner Makran of mostly Eocene to Middle Miocene rocks; *Yellow* Outer Makran of mostly Upper Oligocene to Middle-Miocene rocks; *Light-yellow* Coastal Makran of mostly Upper Miocene and Plio–Pleistocene sediments. Italic = townships in *grey*. **b** Synthetic cross-section along the line indicated in **a**; same colours and legend as in **a**

Geodetic data document a ca. 8 mm/a. current convergence rate between the Makran coast (Chabahar GPS) and stable Eurasia (Vernant et al. 2004). This rate documents on-going, internal shortening of the wedge.

Structural Analysis

Our structural analysis combines field measurements, digital elevation models and interpretation of multi-spectral satellite images to control correlation between cross-sections. The erosional basis of a Late Miocene olistostrome is a major structural reference horizon.

Main Tectono-Stratigraphic Units

The previously published geological maps at 1/250.000 were drafted after time-limited, helicopter-based fieldwork carried out in the 1970s (McCall and Kidd 1982; McCall 1983, 1985, 2002). They provided a substantial reference in terms of stratigraphy and general structure of the onshore MAW. However, our fossil collection and identification revealed some important discrepancies with the published work. Much of this discrepancy with the published maps stems from stratigraphic attributions based on reworked fossils. Our new geological map embraces a representative portion of the MAW exposed in southern Iran. We identified four main tectono-stratigraphic units separated by major thrust zones (Fig. 12.2). From the north to the south, i.e. from top to bottom, these units are:

- *North Makran*, which contains Cretaceous to at least Paleocene deep-marine sediments and volcanic rocks, in part assembled in tectonic "mélanges", the latter term mostly designating complex imbrication zones. Ultramafic rocks were attributed to a Jurassic–Paleocene ophiolitic complex (McCall and Kidd 1982). The tectonically assembled rocks of North Makran were subsequently weakly folded. North Makran likely includes the basement of the southern part of the Jaz Murian to the north (Figs. 12.1, 12.2), which is hidden below sediments. In the south it is floored by the Bashakerd Thrust.
- *Inner Makran* is dominated by Upper Eocene to Lower Miocene terrigenous sandstone–shale sequences of 'flysch'-type conformably overlying (?) Paleocene to Middle Eocene pelagic sediments and volcanic rocks. The 'flysch'-type sediments are thought to be part of a proto-Indus fan recording the Himalayan collision (e.g. Kopp et al., 2000; Ellouz-Zimmermann et al. 2007a; Carter et al. 2010). Folding and thrust-faulting produced growth

structures during Miocene, N–S compression. The unit is confined between the Bashakerd thrust above, and the Ghasr Ghand Thrust below.
- *Outer Makran* exposes mostly Lower–Middle Miocene sediments including deeper-water sandstones and marls, grading up-section into slope and coastal deposits and locally shallow-water limestones. Open and large folds with a weak axial-plane cleavage indicate less shortening than in Inner Makran. This unit is bounded by the Ghasr Ghand Thrust above, and the Chah Khan Thrust below.
- A widespread Tortonian olistostrome (Burg et al. 2008) covers the three previous units.
- *Coastal Makran* comprises Upper Miocene and younger sediments. The sediments of Coastal Makran were obviously deposited in a wedge-top basin with a sequence shallowing from slope marls to coastal and continental deposits. Coastal Makran is very weakly deformed and exposes normal faults not seen in other units. This unit is exposed from the Chah Khan Thrust in the north to the coast.

Other thrusts of secondary importance were mapped in each unit (Fig. 12.2). The major thrusts were recognized from fault structures more intense along their trace, and from major stratigraphic offset that explain the bulk inverted stratigraphy of the area: Cretaceous over Eocene over Oligocene over Miocene. Each of the first-order units has a width of 20–50 km, which is significantly more than the width of imbricates imaged on seismic profiles of the active wedge, which are a few kilometres wide (Grando and McClay 2006). The spacing on seismic profiles would however, correspond to that between second-order thrusts (Fig. 12.2). In the northeast corner of the mapped area, the Bamposht Thrust defines a boundary with folded Eocene sediments whose characteristics make the hanging wall a part of the Sistan system. We did not study this area in details and therefore will not discuss it. We successively describe structural characteristics of each of the four first-order units. Precise stratigraphic analysis is out of the scope of this paper and the relevant data can be found in Dolati (2010).

North Makran

This area mainly consists of Cretaceous igneous rocks and associated sediments and scattered, minor outcrops of Paleocene and Eocene rocks. The oldest dated rocks are pillow lavas and lava flows interlayered with pelagic limestones and hemipelagic marls, red siliceous shales and volcaniclastic sandstones not younger than Barremian (ca. 145–125 Ma, Fig. 12.3). This deep marine association

Fig. 12.3 Lower Cretaceous (pre-Barremian) pillow lavas interbedded with light-coloured hemipelagic limestone and marl at 26° 44′ 02.8″N; 59° 47′ 26.0″E (Fig. 12.2a)

appears to extend into the Upper Cretaceous (Dolati 2010). No continuous stratigraphic sequence could be established; however, a succession of dark grey shales, siliceous limestones, volcaniclastic sandstones and pelagic limestones yielded Campanian nannofossils (Dolati 2010). Locally, Upper Cretaceous shallow-water limestones with rudist fragments and clasts reworked from the Lower Cretaceous volcanics unconformably overlie the Lower Cretaceous submarine volcanic rocks and pelagic limestones (Fig. 12.4), and unconformable Eocene shallow-water limestones are recorded from the boundary with the Jaz Murian (McCall 1985).

We call Imbricate Zone an assemblage of dissociated rock units, in particular serpentinite, gabbro, rare plagiogranite, pillowed and brecciated basalts and radiolarites interpreted as dismembered ophiolites (Desmons and Beccaluva, 1983). This zone has been termed "coloured mélange" by Gansser (1955, 1959; McCall 1983). The main outcrops are located in the northern part of the study area and extend in a northeast-southwest direction, from Pip to near Kahiri (Fig. 12.2a). All studied transects display tectonic slices of few tens to thousands of meter thickness and lateral extension. Lithologies resemble those of the more coherent assemblages of Cretaceous rocks of North Makran. Blueschist slices (Maruyama et al. 1996; McCall 1997) and blocks of marbles are exposed in the northwestern corner of the map. White, thick-bedded to massive recrystallised limestone intercalated within strongly sheared volcaniclastic and basaltic rocks, occur in the basal Bashakerd Thrust

Sheet, the southernmost imbricate of North Makran. Their origin is still enigmatic.

Contact with the Jaz Murian Depression

The contact between the Jaz Murian Depression to the north and the MAW to the south is generally faulted (Fig. 12.2). Rocks of North Makran likely extend further north, as few and small outcrops indicate, but they are largely covered by Jaz Murian Holocene fanglomerates. This imbricate zone is part of the tectonic, "coloured mélange" of McCall (1983) and may delineate either a suture (by reference to ophiolitic fragments and deep-sea oceanic sediments involved in this tectonic zone) or, since every imbricate is allochthonous, be already part of the major backstop against the Tabas Microcontinent, below the Jaz Murian depression (McCall 1997).

The western part of the mapped Jaz Murian boundary is nearly E-W, dominated by normal faults with variable orientations suggesting sub-radial extension (Fig. 12.5a).

The eastern part of the mapped Jaz Murian boundary strikes NE-SW (through Pip and east-south-east of Espakeh, Fig. 12.2a). It mostly consists of NE-SW sinistral strike-slip faults (Fig. 12.5c) associated with NW–SE, conjugate dextral faults and many NW–SE to N–S normal and reverse faults (Fig. 12.5b). Both accommodated nearly N–S shortening. No age determination for either event was possible.

Fig. 12.4 Massive, Upper Cretaceous, rudist-bearing, shallow-water limestones unconformably overlying deep marine limestones with pre-Aptian nannofossils intercalated with pillow lavas. View from 26°43′45.00″N; 59°50′19.4″E (Fig. 12.2a)

Fig. 12.5 **a** Example of fault data from the E-W segment of the Jaz Murian boundary. Measurements in serpentinite within 100 m north and south of GPS points: 26°54′42.9″N; 59°29′4.68″E. **b** Example of fault data along the SW-NE contact of Jaz Murian. Faults measured in basalts within 100 m to the SW and NE of GPS points 26°53′1.62″N; 60°26′0.6″E. Equal area, lower hemisphere; *arrows* indicate the movement direction of the hanging wall. **c** Calcite fibres indicating sinistral movement on an 80°NW-dipping fault plane of the Jaz Murian boundary; GPS point: 26°51′57.48″N; 60° 24′ 14.7″E (Fig. 12.2a)
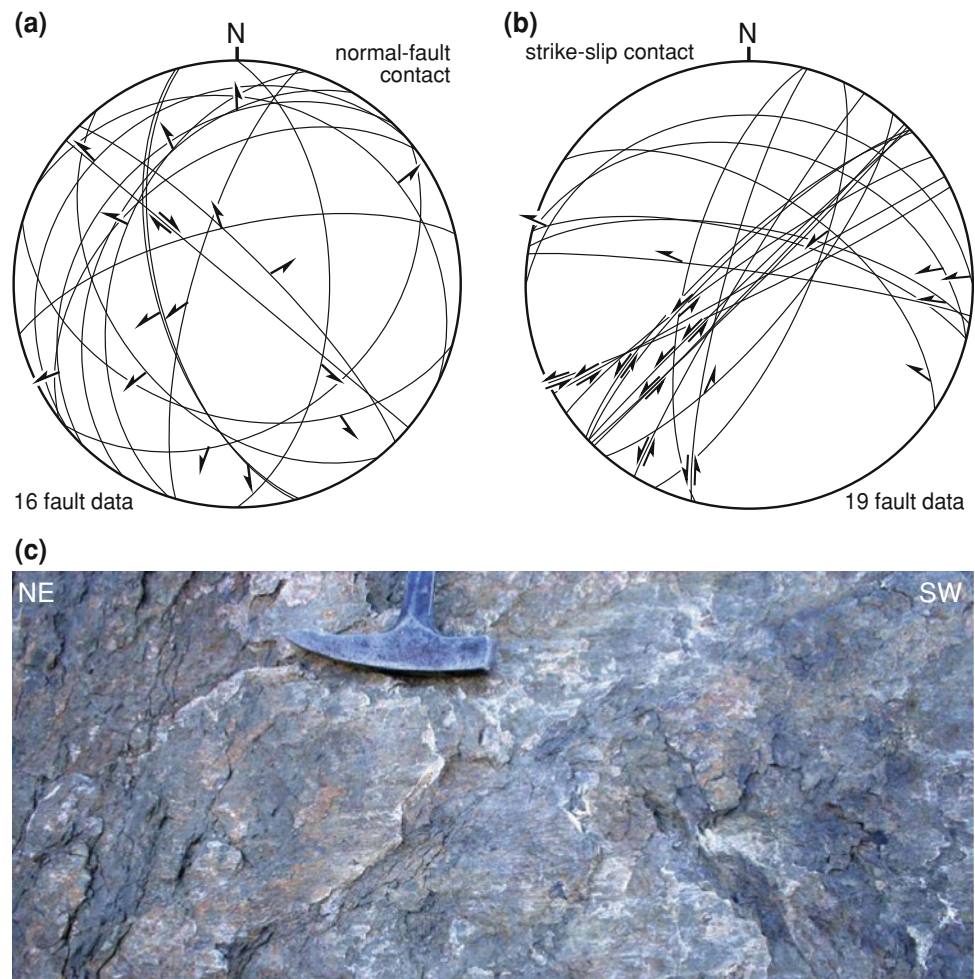
N–S shortening deduced from conjugate strike-slip faults along the SW-NE Jaz Murian boundary contrasts with radial to N–S extension along the E-W segment of this boundary. This discrepancy suggests different faulting events whose time relationship could not be established.

Imbricate Zone

The Imbricate Zone occurs in two places (Fig. 12.2a):

1. To the north (top-left corner of Fig. 12.2a), S-dipping, important backthrusts (Fig. 12.6) separate lavas and
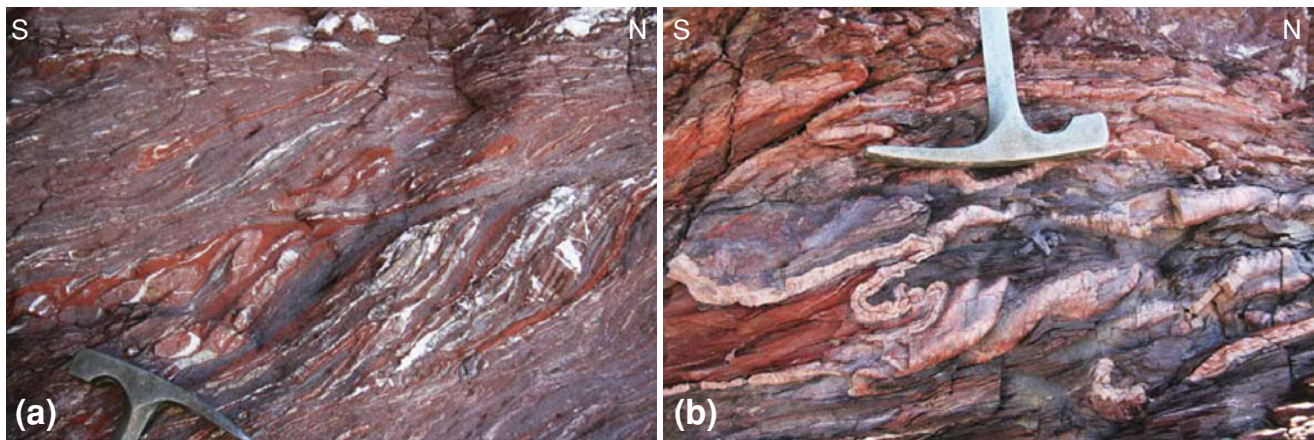
Fig. 12.6 Evidence for top-to-the-north back-thrusting in the Imbricate Zone of North-Makran: **a** sigmoidal rock lenses, shear bands and N-vergent drag folds at 26°50′51.3″N; 59°31′38.1″E (Fig. 12.2a); **b** Non-cylindrical to sheath folds at 26′52.0″N; 59°31′40.6″E (Fig. 12.2a). Both outcrops in probably (facies correlation) Upper Cretaceous red shales
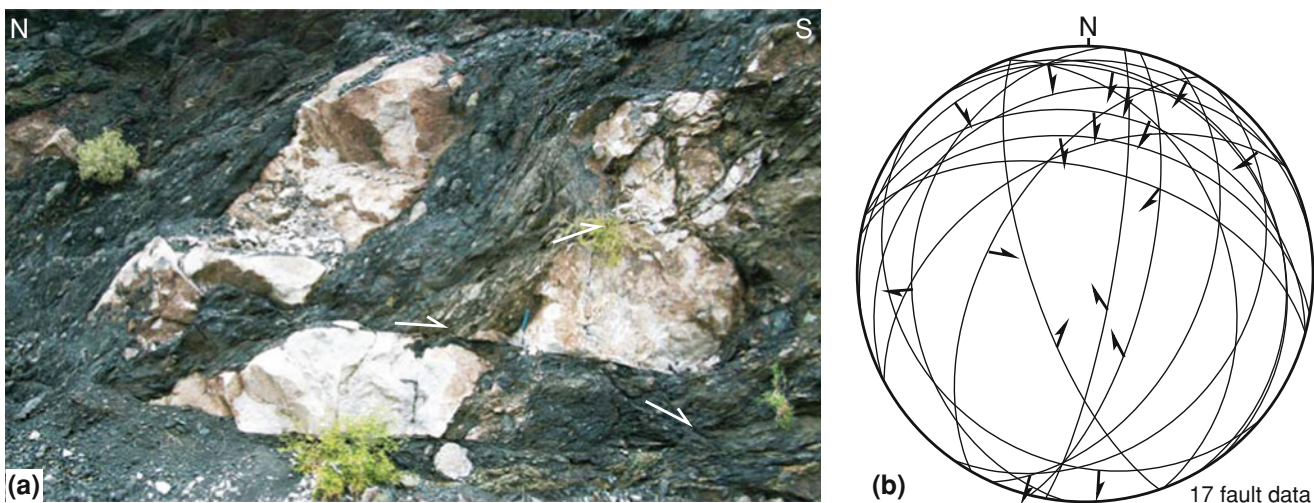
Fig. 12.7 a Bashakerd thrust zone at GPS: 26°32′11.7″N; 59°38′26.6″E. Sheared blocks of white marble in the highly sheared matrix of *dark grey* volcaniclastic sandstone. Top-to-the south movement (*white arrows*) defined from offset marble blocks and sigmoidal foliations in matrix. Note association of north- and south-dipping (hinterland-dipping, foreland-dipping, respectively) shears building the anastomosing system of fault zones. **b** Fault data from the Bashakerd thrust zone within 100 m north and south of GPS point 26°32′6.36″N; 59°38′20.58″E. Same projection and symbols as Fig 12.5

sediments of N-Makran from the footwall, Imbricate Zone.

2. To the south, the N-dipping Bashakerd Thrust Zone separates North-Makran from the footwall Inner Makran.

In the north, the Imbricate Zone is mostly exposed outside the study area, to the west, so that not enough measurements have been taken to make a solid interpretation. At the moment, the position of polyphase metamorphic slices (including the blueschists) remains questioned as to whether they occur in a klippe or as part of an anticlinal stack exposing ophiolitic slivers from a deep duplex structure as in modern accretionary wedges (e.g. Bernstein-Taylor et al. 1992). Faults between the individual tectonic slices are usually north-dipping, south-vergent thrusts.

The Bashakerd Thrust Zone brings Cretaceous rocks onto Eocene turbidites. The thrust can be traced westward on satellite images up to the Minab Fault that separates the MAW from the Zagros Mountain Belt (Fig. 12.1). Eastward, near Pip, the Bashakerd Thrust Zone is offset by the SW-NE segment of the Jaz-Murian Boundary and is difficult to identify further east, perhaps because it runs through or is covered by the olistostrome (Fig. 12.2a).
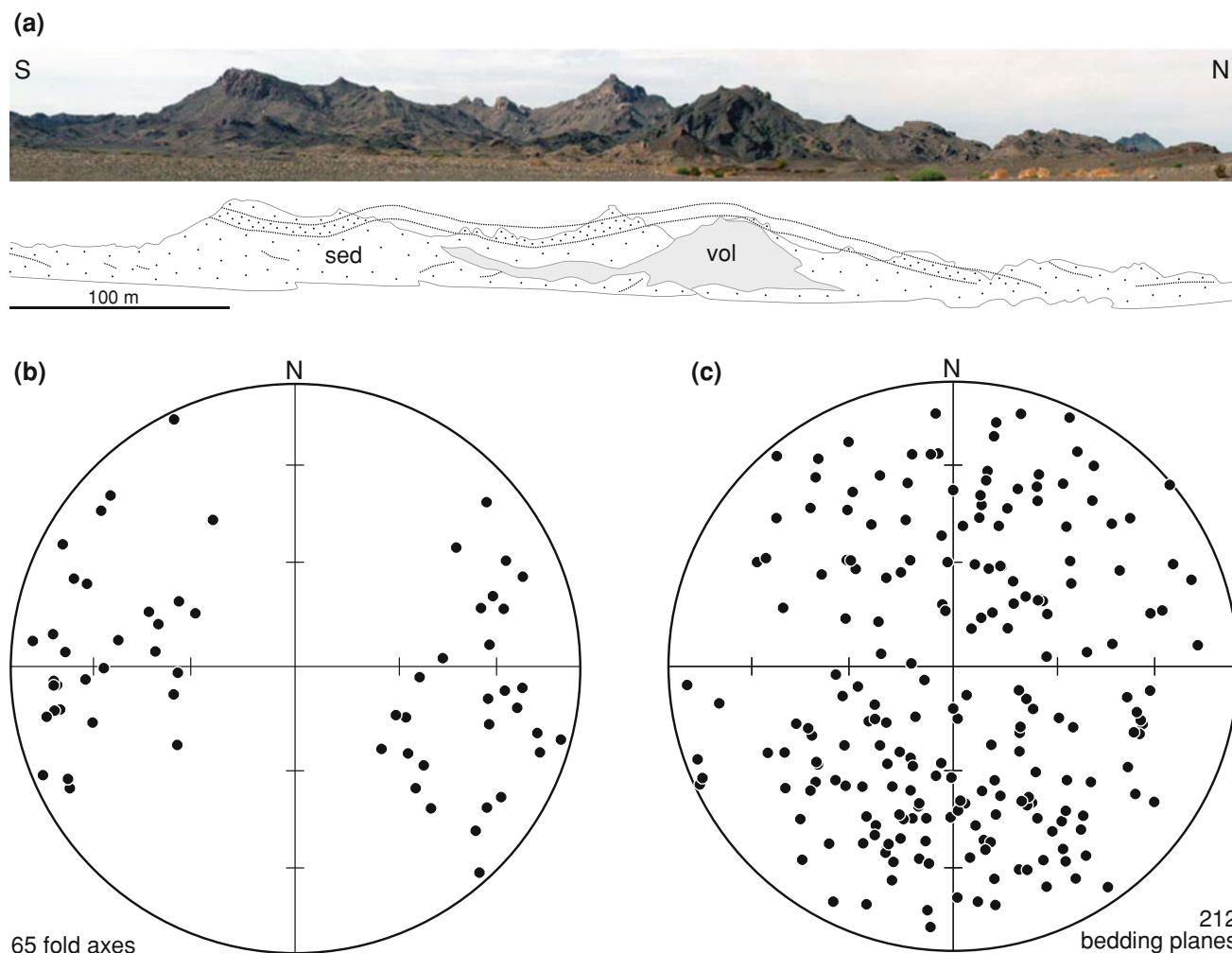
(a)

(b)

65 fold axes

(c)

212
bedding planes

Fig. 12.8 **a** Panorama (*top*) and sketched legend (*bottom*) of a typical large-wavelength fold in Lower Cretaceous sediments (*sed*) and volcanic rocks (*vol*) of North-Makran. Picture taken from

26°45′16.7″N; 59°52′34.8″E (Fig. 12.2). **b** and **c**: Equal area, lower hemisphere projection of structural measurements in North-Makran

The best exposed outcrops of the Bashakerd Thrust Zone are located south of Fannuj (Fig. 12.2a), where it has an approximate thickness of 500–700 m. There, the fault zone contains blocks of white marble in dark grey volcaniclastic sandstone, lavas and few red shales (Fig. 12.7a). The number of marble blocks apparently increases northward. The hanging wall North-Makran unit exposes similar marbles, which makes it a possible source. The strongly deformed matrix (Fig. 12.7a) suggests tectonic incorporation of the blocks into the thrust zone. This sheared matrix shows a marked foliation with a general orientation N 100–50 N, subparallel to the longest axis of the variably sized and chaotically occurring marble blocks. Changes in dip of the foliation toward fault planes delineate sigmoidal patterns which, along with the lens shape of marble blocks, indicate a general top-to-south movement (Fig. 12.7a).

Measurements of fault planes and slicken lines (Fig. 12.7b) indicate that the main fault planes are N- to

NE-dipping reverse faults associated with a few S-dipping reverse faults. Shallow (20–30°) S-dipping faults with top-to-south movements are frequent (Fig. 12.7a and b). Both N- and S-dipping, south-verging faults make an anastomosing pattern that cuts and wraps the marble blocks.

Structures within North-Makran

Structures within the North-Makran thrust sheet are essentially thrusts, folds and faults.

Detailed measurements and cross sections reveal generally open folds with a large (>200 m) wavelength (Fig. 12.8a). They trend nearly E-W (Fig. 12.8b and c). Axial plane foliations are weak and in many cases nonexistent. These fold characteristics reflect the generally weak deformation. However, a foliation occurs to the south and increases in intensity southwards, towards the

Bashakerd Thrust Zone. This foliation indicates increasing strain towards the basal thrust and is thus independent of folds within the sheet.

Inner Makran

The oldest dated rocks in Inner Makran are Lower–Middle Eocene deeper-marine pelagic/hemipelagic, mostly red limestones and marls with intercalated volcaniclastics, redeposited by mass-flow processes, and, occasionally pillowed volcanic rocks. Above this, siltstones and graded fine sandstones pass up-section into an Upper Eocene–Upper Oligocene upward-thickening and -coarsening turbiditic succession recording the progradation of a sub-marine fan system. Qayyum et al. (1996) suggested that this system was part of a proto-Indus deep-sea fan that had its main source area in the India–Asia collision zone. Indeed, the sandstone composition reflects a recycled orogenic source in addition to volcanic detritus (Critelli et al. 1990) compatible with this interpretation (Carter et al. 2010). At places, crudely graded conglomerates with ophiolitic clasts, well-preserved nummulitids and alveolinids (not younger than Middle Eocene) testify to an area in the north or northeast where ophiolites were exposed and shallow-water carbonate sediments deposited. In the north, the succession shallows through thin-bedded, shale-rich pro-delta turbidites (Upper Oligocene) to shelfal sandstones deposited under the influence of waves and tidal currents (Dolati 2010). Air-fall ash layers, testify to volcanic activity during Eocene and Early Oligocene times. In the southern part of Inner Makran,

deeper-marine, turbiditic sedimentation persisted into the Middle Miocene (Ghasr Gand Thrust Sheet).

Structural Subdivision

Six thrust sheets have been distinguished, from top to bottom (Fig. 12.2a):

- The Lashar and Chanf Thrust Sheets contain mainly Eocene to Oligocene turbidite successions. The Lashar Thrust Sheet is the western lateral equivalent of the Chanf Thrust Sheet, to the east, offset by sinistral faults of the Jaz Murian boundary.
- The Pishamak Thrust Sheet is the eastern equivalent of the Kajeh Thrust Sheet. The outcrop areas of the thrust sheets are separated by a large outcrop of olistostrome and contain mainly Oligocene turbidite successions with fewer Lower Miocene sediments in the Pishamak Thrust Sheet.
- The Ghasr Ghand Thrust Sheet and the Kahorkan Thrust Sheet are the lowermost units of Inner Makran in the eastern and western parts of the study area, respectively. They expose Oligocene to Middle Miocene sediments.

Structures

A moderate to strong cleavage characterizes all outcrops of Inner Makran (Fig. 12.9). This very low grade cleavage is axial plane to variably shaped folds (open box folds to tight chevron folds) generally trending NW–SE and plunging
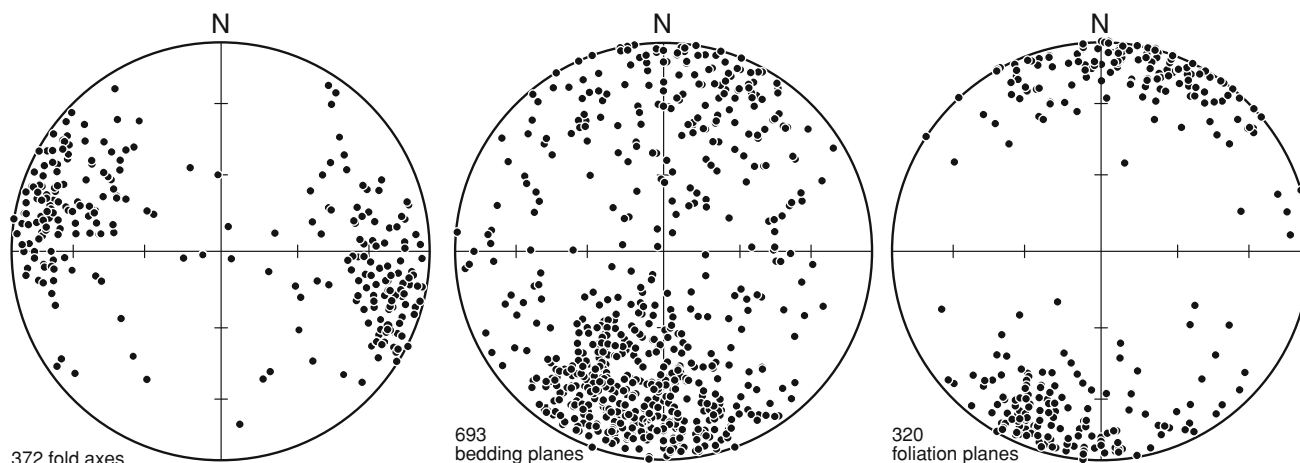
Fig. 12.10 *Lower hemisphere*, equal area projection of structural measurements in Inner Makran

shallowly to steeply in either direction (Fig. 12.10). Their wavelengths depend on the competence and thickness of the involved layers. Large-scale fold axes can be followed for hundred meters to several kilometres, denoting cylindricity and large lateral extent of major structures. The cleavage does not bear any prominent stretching lineation. However, calcite fibres between segments of boudinaged sandstone layers in fold limbs show a regionally consistent stretching direction (015–025) nearly orthogonal to fold axes. Many bedding planes bear striations and mineral fibres also nearly orthogonal to the local fold axes. Opposed senses of movements on successive fold limbs indicate that bedding-parallel slip surfaces represent flexural-slip folding (e.g. Ramsay and Huber 1987) rather than bedding-parallel thrust surfaces.

In different places, changes in thickness and dip of Middle Miocene strata and intraformational unconformities define growth structures (Fig. 12.11). They indicate folding and thrusting during Middle Miocene sedimentation, in particular along the Ghasr Ghand Thrust.

Strata-parallel faults, footwall flats–hanging wall ramps (Fig. 12.12a) and hanging wall flats–footwall ramps (Fig. 12b), demonstrate flat-and-ramp systems. In this tectonic style, many south-vergent, asymmetric folds, with steep to overturned forelimbs cut off by ramp faults are interpreted as fault-propagation folds. Together, these structures are the basis for associating major folds to ramp systems on cross-sections. Large anticlines are likewise ramp-anticlines. If in itself this is not a fundamental discovery in an accretionary wedge, we emphasize that the cleavage present everywhere, and intense folding, depart from the traditional Coulomb-wedge assumption of faulting without strain.

It is sometimes difficult to identify thrust faults of regional significance, and distinguish them from subordinate reverse, fold-propagation faults and thrusts that accommodate disharmonies inherent to tight folding. Indeed, faulted fold limbs are common in the region; yet, the relative displacement dying out within a few meters along the fault plane demonstrates that such faults are local mechanical instabilities due to excess tightening of hinge zones. In some places, tilted flats and ramp systems suggest that earliest movement planes may have been folded and foliated along with the sediments that contain them. These possibly folded thrust zones require further, very detailed mapping we could not carry out.

A few N–S trending folds were mapped to the south of Chanf and Kahiri (Fig. 12.2a). They might indicate folding in the footwall of the Bamposht Thrust (top right corner of Fig. 12.2a) at the front of the Sistan Mountain Range (Fig. 12.1). Since we could not find interference patterns, we presently interpret these folds as disharmonic features within tight closures of larger folds.

Thrust Zones

Major and subsidiary thrust zones are identified from stratigraphic repetition. Major thrusts are thicker and highly sheared zones with intense foliation in asymmetric, tight, fault-related folds. Measurements of fault planes and slicken lines demonstrate shallowly, NE- to NW-dipping reverse faults associated with conjugate, S-dipping reverse faults to the south of Fannuj (Fig. 12.13). All measurement sites exhibit bulk southward thrusting.

The Ghasr Ghand Thrust is one of the most important faults of the study area. Its trace can be followed on satellite images over a length of more than 250 km in E–W direction up to the north of Turbat in Pakistan. Upper Oligocene

Fig. 12.11 Growth structure in Middle Miocene turbidites, at 26°19′27.78″N; 60°23′17.04″E (Fig. 12.2a). The fanning, wedge-shaped geometry of growth strata indicates synsedimentary limb rotation

Fig. 12.12 a Footwall flat–hanging wall ramp in Upper Oligocene (Chattian) turbidites; splay from the Kajeh Thrust (Fig. 12.2a) at 26°23′26.2″N; 60°27′52.3″E; **b** hanging wall flat–footwall ramps of a splay of the Kahorkan thrust (Fig. 12.2a) within Oligocene sandstones, seen from 26°16′54.0″N; 60°10′25.7″E

turbidites placed onto tilted Pliocene–Pleistocene conglomerates indicate recent thrusting between Ghasr Ghand and Pishin (Fig. 12.2a). Despite this obvious sign for multiple activations, until recent time, fault data along the thrust zone do not display any significant difference of fault kinematics (Fig. 12.14).
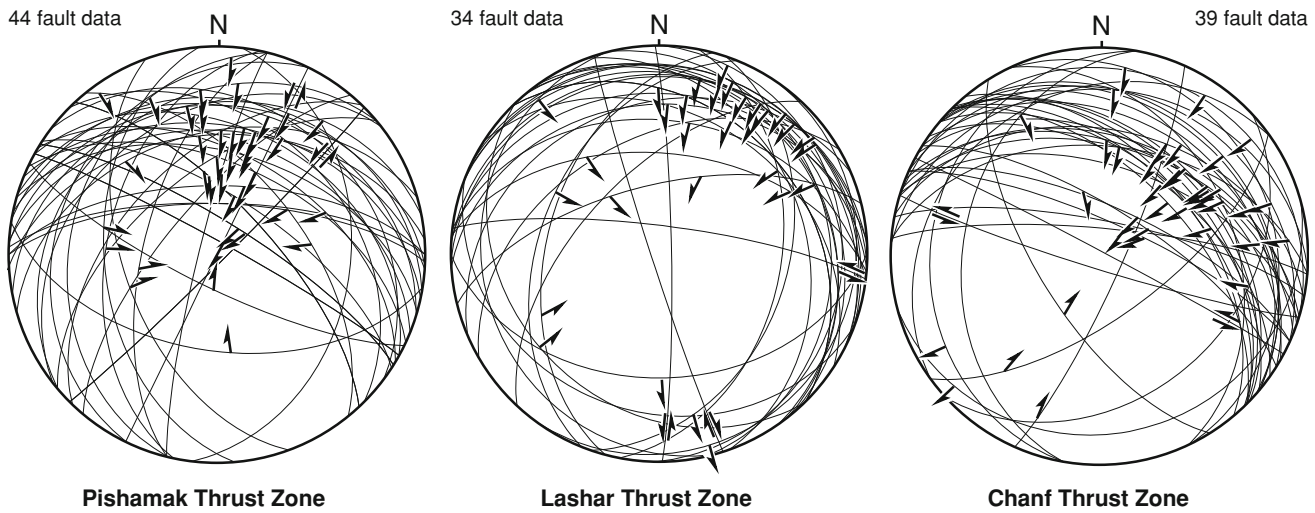
Fig. 12.13 Fault data measured along the intermediate thrust zones within Inner Makran (Fig. 12.2a). Same projection and symbols as Fig. 12.5
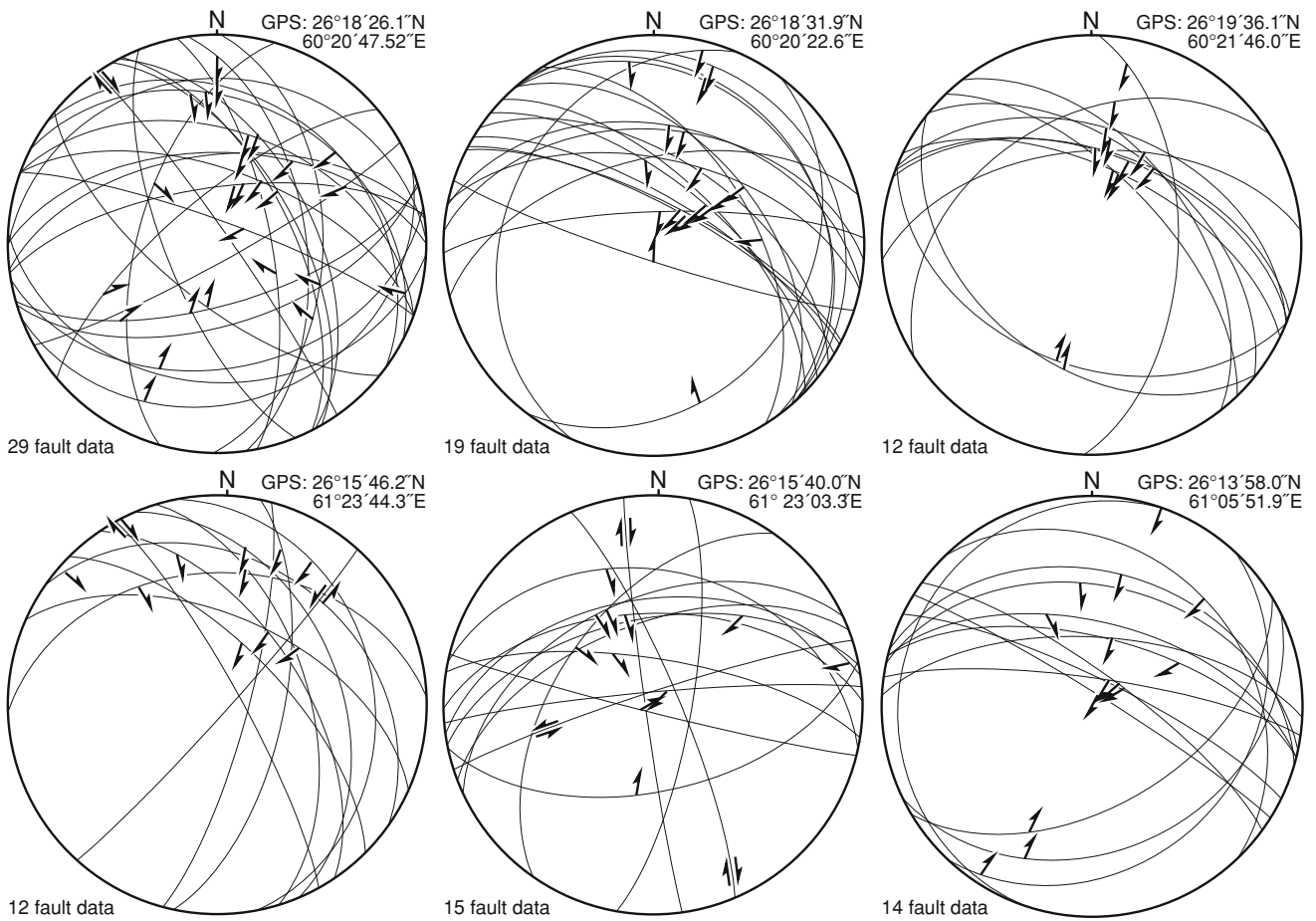

Fig. 12.14 Fault data measured along the Ghasr Ghand thrust zone (Fig. 12.2a). Same projection and symbols as Fig. 12.5
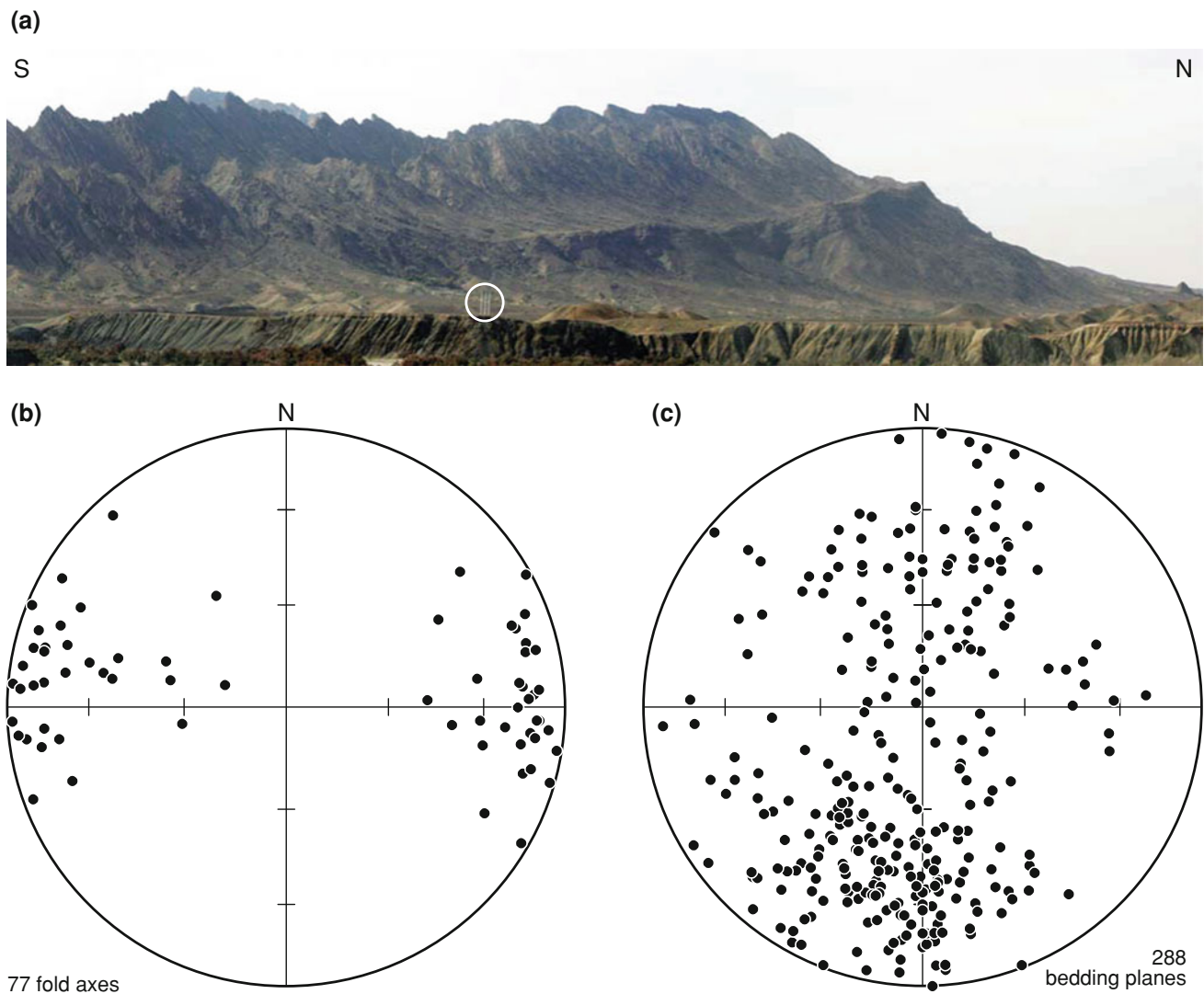
(a)

(b)

77 fold axes

(c)

288 bedding planes

Fig. 12.15 **a** Large rounded syncline folding sandstone-dominated Lower Miocene sediments of Outer Makran at 26°15′35.28″N; 60°10′45.12″E (Fig. 12.2a). Electric poles (*circled*) as scale. **b** and **c** Equal area, lower hemisphere projection of structural measurements in Outer Makran
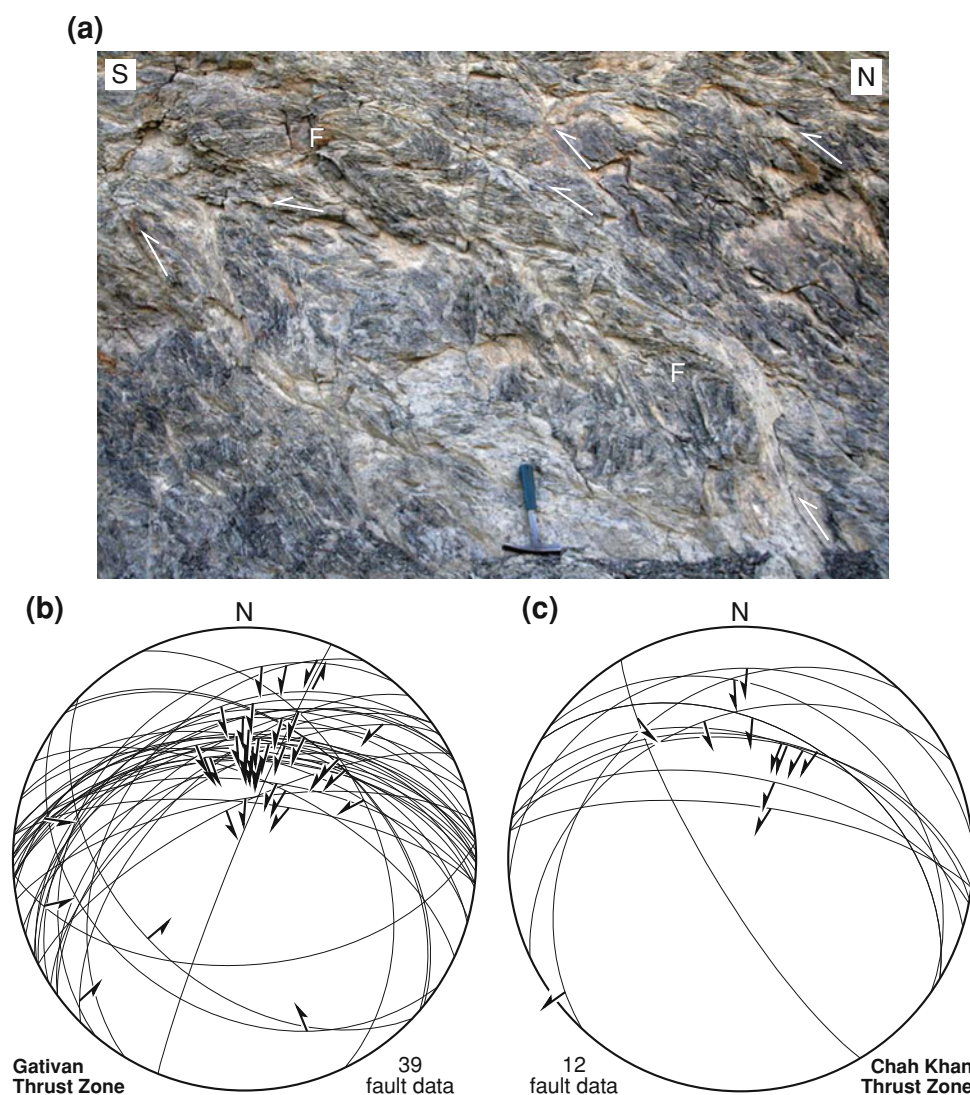
Strike-Slip Faults

Sub-vertical (dip > 80°) strike-slip faults, readily visible on satellite images, are particularly abundant in Inner Makran (Fig. 12.2a). NE–SW sinistral strike slip faults that have a topographic signature define the largely dominant set. NNW–SSE, less common dextral faults that also shape the topography are conjugate. These likely very recent faults define a bulk NNE–SSW shortening, consistent with the known convergence direction between Iran and the Arabian Plate.

Some strike-slip faults, however, die out rapidly along their length and appear to have transferred displacement onto EW-trending thrusts and folds. These transfer faults would be contemporaneous with the older folding-thrusting event that structured the MAW.

Outer Makran

Outer Makran exposes mainly Lower Miocene to Middle Miocene sediments overlying Upper Oligocene turbidites and shales. They form two thrust sheets, Gativan in the north and Chah Khan in the south (Fig. 12.2). In the more internal Gativan Thrust Sheet, the Lower Miocene formations consist of siltstones and marls with calcareous sandstones in which secondary gypsum veins are ubiquitous. They were probably deposited in a slightly hypersaline basin with a restricted circulation. Patchy mounds of reefal, coral-algal limestone of Burdigalian age confirm shallow-water environments (McCall 1985; McCall et al. 1994). The overlying Middle Miocene clastic sequences are arranged in upward- thickening and -shallowing cycles representing slope to near-shore and shoreline deposits. In the more

Fig. 12.16 a Gativan thrust zone: strongly sheared (*arrows* next to some of the anastomosing shear planes point to sense of shear) and folded (*F*) Mid-Miocene shales. Outcrop at 26° 05′10.4″N; 60°58′38.2″E (Fig. 12.2a). **b** Fault data distributed along the Gativan Thrust within Outer Makran (Fig. 12.2) and **c** on the basal Chah Khan Thrust Zone, 100 m north and south of GPS point 25°53′42.4″N; 60°36′16.2″E. Same stereo projection and symbols as Fig. 12.5

Structures

Cross sections and measurements show essentially symmetric, open to gentle, rounded to box folds (Fig. 12.15a) with large (>1,000 m) wavelength in both the Gativan and Chah Khan Thrust Sheets. These folds trend roughly E–W and plunge shallowly in either direction (Fig. 12.15b and c). This fold style, along with the weak/absent axial-plane foliation, reflects only weak deformation. However, such large, parallel folds are normally associated with deeper décollement surface(s) (e.g. Jamison 1987; Sepehr et al. 2006).

external Chah Khan Thrust Sheet deeper-marine shales and marls interspersed with turbiditic sandstones persist into the Middle Miocene.

Thrust Zones

The intermediate Gativan Thrust is a 300–400 m thick zone best exposed to the southeast of Ghasr Ghand (Fig. 12.2a). A densely anastomosing pattern of N-dipping reverse faults dissect dark grey shales with strong foliations refolded around drag folds in lens-shaped elements. Deflection of foliation planes toward and into the fault planes delineates a sigmoidal pattern that indicates a bulk top-to-south-south-west movement (Fig. 12.16a). S-vergent drag folds are consistent with this thrusting direction (Fig. 12.16 b). Such structures are nowhere as spectacular in other places of Outer Makran, which indicates that the Gativan Thrust is one of the major faults of the study area and that the deformed Middle Miocene shales are a potential detachment horizon.

The basal Chah Khan Thrust Zone is less than 100 m thick. S-vergent folds in its footwall and not seen elsewhere in Coastal Makran are interpreted as fault-propagation folds. Measurements of fault planes and slicken lines indicate movement of the hanging wall towards the south-southwest (Fig. 12.16c).

Olistostrome

The Tortonian olistostrome covers North- Inner- and Outer-Makran unconformably (Fig. 12.2a). It typically shows a chaotic mixture of dissociated turbidites with a non-metamorphic, muddy, shaly matrix including randomly mixed blocks of various composition (limestones, sandstones, shales, chert, schist, pillow lava, mafic to ultramafic rocks), shapes (rounded and angular) and sizes (mm to km across). This olistostrome is matrix-supported with a matrix of pebbly mudstone. At places, the varicoloured matrix displays a weak scaly fabric. The physical and lithological characteristics change from north to south, with larger and older exotic blocks more abundant in the north. Most exotic blocks in the south are sandstones similar to, and therefore probably scrapped off from sandstones of the underlying turbidites.

Few occurrences of the olistostrome in Coastal Makran form the eroded cores of anticlines exposing the upper stratigraphic boundary of the olistostrome, which is a microconglomerate to coarse sandstone unit. The stratigraphic age of the olistostrome is well constrained by its stratigraphic relations with the under- and overlying sequences. Internally, it rests unconformably on folded and eroded early Tortonian turbidites (ca. 11.6 Ma). An upper age bracket is given by the ca. 9.6 Ma old Tortonian marls covering the olistostrome.

The olistostrome is interpreted as a mud-and-debris flow deposited during a single catastrophic event (Burg et al. 2008). Its erosive base makes therefore an excellent time reference.

Structures

The olistostrome is largely covering several thrust units along with the thrust zones that separate them. In North Makran, the olistostrome is unconformable on the Imbricate Zone north and west of Kahiri (Fig. 12.2a) and includes large olistoliths derived from the Imbricate Zone. This indicates that the Imbricate Zone became involved in the mass wasting that down-slope covered the relief the head of the flow had eroded. Like many gravitational mass-wasting events, it might have been triggered by earthquakes related to tectonic movements. In some places as SE of Espakeh,

the Imbricate Zone is thrust onto the olistostrome. Such observations indicate late Neogene reactivation of thrusts after emplacement of the olistostrome.

A weak spaced cleavage in the shaly olistostrome matrix has the same attitude as the axial plane cleavage of folds in the underlying sequences, which attests to post-olistostrome folding by E–W folds concordant with the tight folds in the underlying sequences; however, folds are tighter in the underlying sequences and are cut by the olistostrome, which therefore appears to represent an event overlapping with regional folding and thrusting.

Connecting and correlating thrust planes through the olistostrome is not straightforward because fault zones within the mud-dominated matrix are difficult to detect and track for long distances. However, detailed mapping on contact areas makes us confidents that some as the Kajeh Thrust (Fig. 12.2a) are sealed by the olistostrome and therefore were not reactivated after the olistostrome emplacement. The irregular distribution of folds and thrusts affecting the olistostrome is attributed to the rheological changes induced by the sudden load of the olistostrome on the wedge (Smit et al. 2010).

Coastal Makran

Coastal Makran exposes Upper Miocene marls with minor calcareous sandstone interbeds increasing up-section. These slope marls, of Tortonian–Messinian age, grade up-section into sequences arranged in upward-thickening and -shallowing cycles of Pliocene shelfal, near-shore to shoreline deposits. Inland, fluvial conglomerates and sandstones and, near the coast, marine sandstones and marls with intercalated calcareous bioclastic sandstones unconformably overlie the older deposits. Pleistocene fluvial conglomerates occurring along the coast and topped by marine erosional surfaces testify to young tectonic uplift.

Folds

It almost needs systematic bedding measurements to unravel the open-gentle, rounded-blunt folds with very long wavelengths (>10 km) and low amplitudes that affect the Upper Miocene–Pliocene sequences. Fold axes trend nearly E–W for several kilometres with axes plunging shallowly in either directions (Fig. 12.17).

Normal Faults

Normal faults cutting sediments younger than Late Miocene (Fig. 12.18a and b) are the remarkable structures in a band

43 fold axes

163
bedding planes
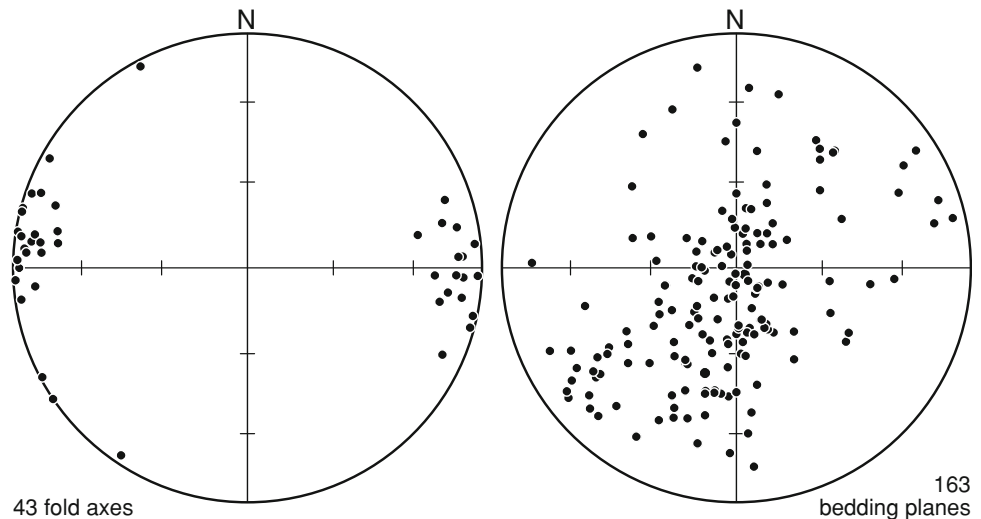
that does not extend more than few kilometres northward
from the coast. These usually planar faults are likely anal-
ogous to those that offset Pliocene–Pleistocene shelf
sequences in offshore seismic sections (e.g. Harms et al.
1984; Platt et al. 1985; Grando and McClay 2006). They
express extension (Hosseini-Barzi and Talbot 2003), likely
responsible also for sediment-filled fractures (Fig. 12.18b).
Active mud volcanoes (e.g. Schlüter et al. 2002) are spa-
tially related to the normal faults. Detailed record from
Plio–Pleistocene marine sediments logged onshore, along
the coast, suggests that some normal faults have been epi-
sodically inverted during sedimentation (Hosseini-Barzi and
Talbot 2003).

Discussion

General Structure

Most of the sediments involved in the successive thrust
sheets are very low grade, which indicates that they were
never buried below thrust sheets that would have been
eroded since then. As a matter of fact, the fission-track ages
of apatite mineral grains from Inner Makran to the coast
have not or only partly been reset, showing that tempera-
tures never exceeded ∼110 °C, i.e. 5–6 km burial,
assuming a low geothermal of ∼20 °C.km^{-1} (Dolati 2010).

The Bashakerd Thrust is the major tectonic contact
separating two geologically different domains. In its foot-
wall, from Inner Makran to the south, we documented a
fold-and-thrust belt that constitutes the upper part of the
MAW. In the hanging wall, imbricates have a different
tectonic history with obduction of ophiolites in the latest
Cretaceous and early Tertiary as indicated by the associated
unconformities (e.g. Fig. 12.4). The lacking evidence for
large-scale overthrusting raises the problem of the origin

and emplacement of the blueschists and other metamorphic
rocks in the Imbricate Zone. They either represent the
frontal tip of a thrust rooted in the back-stop, below the
Quaternary sediments of the Jaz-Murian, or were exhumed
from below in an anticlinal stack. More structural work, to
the west of the study area, is needed to answer this point and
to elucidate the exact age and tectonic significance of the
late Cretaceous unconformity observed within North-
Makran. The occurrence of mafic and ultramafic clasts
together with reworked nummulitids in deep-water con-
glomerates in Inner Makran testifies that North Makran had
undergone ophiolite obduction, deformation and erosion
before the Early Eocene.

In the fold-and-thrust belt, regionally distributed, E-W
folding and associated flat-and-ramp structures denote the
bulk N–S shortening expected from the continued northward
subduction of the Tethys ocean floor below Iran. Complex
interplay between folding and thrusting with contemporane-
ous foliations involves more internal strain than theories of
accretionary wedges envision. Although there is a clear
change of structural style between intense folding in the
Eocene–Middle Miocene turbidites and broad buckling of the
Upper Miocene–Pliocene sediments, we could not find
evidence of successive "folding phases" in the older sedi-
ments. Continuity of cleavage surfaces across the erosive
basis of the olistostrome, consistency of orientation at a
regional scale and the lack of superposed folds and cleavages
suggest that pervasive axial plane cleavage in the Eocene–
Early Miocene turbidites and spaced cleavage in the shaly
matrix of the olistostrome represent the same stage of
deformation whose development included the time of
emplacement of the olistostrome. The difference in fabric
intensity reflects a difference in amount of folding through
time whereas the lack of superposed folds or cleavages sug-
gests, along with the consistency of structural orientations,
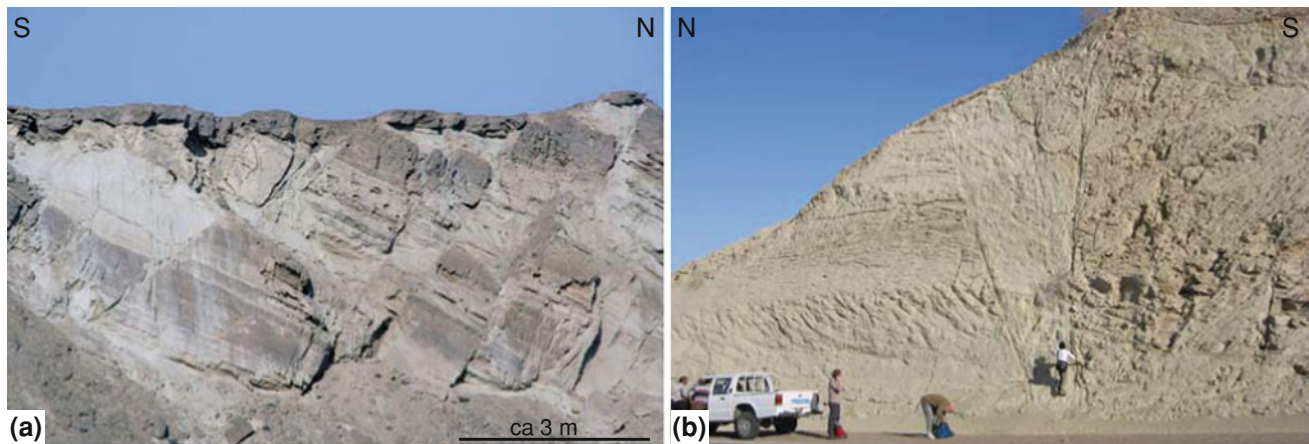continuous and homoaxial folding. The conspicuous

Fig. 12.18 Normal faults in Coastal Makran. **a** Bookshelf faults in Lower Pliocene sediments capped by Plio–Pleistocene gravels at 25°15′40.68″N; 60°49′41.58″E (Fig. 12.2a). **b** Normal faults and sediment-filled fracture at 20′46′86″N; 60°36′51.78″E (Fig. 12.2a)
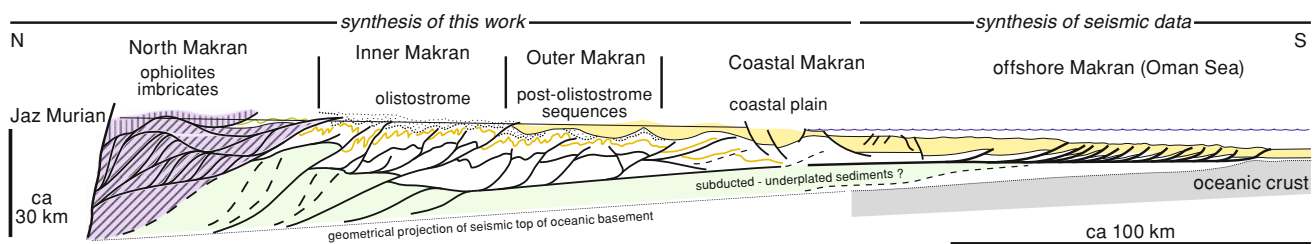

Fig. 12.19 General, synthetic profile across the Makran accretionary system. The active, offshore accretionary wedge is drawn using seismic profile and interpretations of Fig. 12.7 in Grando and McClay (2006). The subducted oceanic crust, underplated sediments and Makran décollement are from seismic profiles of Kopp et al. (2000)

dissimilarity in folding style between ample buckling of Upper Miocene sequences in Outer and Coastal Makran and the tight chevron folding of the older sequences represents more than decoupling and/or disharmony between infra- and superstructures. We conclude that E-W folding began in Early to Middle Miocene times during turbiditic sedimentation (growth structures up into Middle Miocene) and continued until the Upper Pliocene fanglomerates unconformably covered the region and sealed the structures. This interpretation implies very large scale "growth" structures with small angular variations from bed to bed, building sedimentary wedges comparable to those imaged in offshore seismic profiles (e.g. Kopp et al. 2000; Grando and McClay 2006); these occur over several kilometres and thus are not observed easily in the field.

Inferring thin-skin tectonics raises the question of which stratigraphic levels were décollement horizons. Middle Miocene shales, described in the Gativan Thrust Zone are one. We place another décollement in the very thick Upper Oligocene shales sampled by mud volcanoes of Coastal Makran. These two levels should define a duplex structure at the wedge scale, but erosion has not reached deep enough

to allow direct observation. Multiplicity of décollement horizons likely makes the general structure of an accretionary wedge more complex than the usual picture of a series of splay faults branching off and ramping sequentially from one main décollement at the plate interface. Elevated topography of non-buried sediments at the back of the MAW system suggests surface uplift. We speculate that this happens above blind imbrication. Stacking of deep geological units will push up the overlying rock units that consequently escape deep burial despite important shortening. The pre-olistostrome accretionary wedge and its décollement(s) should consequently be deformed by younger tectonic subcretion; post-olistostrome, out-of-sequence thrusts or thrust reactivation, such as on the Ghasr Ghand Thrust (Fig. 12.2), likely sole out to one or rather two subcreting décollement levels, one mid-crustal and the other along the oceanic crust/sediment boundary. This general consideration has oriented the structural interpretation illustrated in Figs. 12.2b and 12.19. Geometrical continuation of offshore seismic data places the active décollement surface at 10−15 km depth below Inner Makran (Fig. 12.19). Besides reactivating splay faults like

the Ghasr Ghand Thrust other consequences of the deep, subcreting and active décollement should be folding and faulting of older duplex structures in the hanging wall.

Age of Deformation

Our study shows that there is no evidence of deformation and regional erosion south of North Makran before the Late Oligocene–Early Miocene. If there is an early, Paleogene wedge as inferred for the Pakistan segment of Makran (Platt et al. 1988), it would be in the Imbricate zone and further north, below the Jaz Murian Basin. The Tortonian olistostrome and the growth structures in Mid-Miocene turbidites place important time constraints on the structural development of the MAW. The emplacement of the olistostrome was an instantaneous and massive mass redistribution that influenced the thrust-wedge mechanics leading eventually to a shift of thrust imbrication to the frontal offshore part of the wedge limiting out-of-sequence thrusting in the inboard part of the MAW (Smit et al. 2010). Yet, regional cleavage and folding denotes significant and distributed shortening after emplacement of the olistostrome.

Protracted Deformation

South of North Makran, we face the lack of evidence for long-lived, continuous, progressive southward migration of folding/thrusting from the Cretaceous or the Eocene to Recent time, as would be expected in in-sequence imbrication of the wedge. We conclude that distributed shortening was an important mechanism during the structural evolution of the accretionary complex, taking place synchronously on several fold and thrust sites, with strain partition between disharmonic buckling, fault-propagation folding and thrust displacement. Why is shortening from Inner Makran to the coast apparently bracketed everywhere between ca. 25 and 4 Ma while subduction below the wedge was continuously active since at least the Late Cretaceous? Folds in the older sequences are very tight and, along with the associated cleavage, represent ca. 60 % shortening by simply unfolding the sections we mapped out in details (Dolati 2010). Accepting 2 cm.a^{-1} subduction rate in the Gulf of Oman (McQuarrie et al. 2003; Bayer et al. 2006; Vigny et al. 2006), we obtain ca 240 km plate convergence during the folding period, while 60 % shortening by folding would have absorbed ca. 235 km over the 350 km wide Tertiary wedge. This startlingly good fit suggests that, while there was subduction with no deformation south of the "coloured mélange" of the North-Makran from Eocene to Early Miocene, there was a period of deformation that nearly compensated all of the plate convergence from Early

Miocene to Pliocene, before deformation was shifted to the modern, distal wedge. A corollary of this simple calculation is that there is a major décollement surface between the folded onshore MAW and the subducting plate that carried away its basement. Back to the within-wedge duplex discussed above, one may speculate whether the exposed MAW is a pre-duplex accretionary wedge while the active offshore Makran represents a post-duplex phase of accretion.

Why is protracted folding and faulting so limited in time? More than any process inherent to the subduction system, we have to consider that an external factor triggered deformation of the wedge. One may wonder, for example, whether folding and thrusting were not prompted by changes in plate kinematics, since spreading in the Gulf of Aden began nearly synchronously in the early Middle Miocene (17–18 Ma, Leroy et al. 2004). The related reorganisation of plate boundaries is an important event that Ellouz-Zimmermann et al. (2007a) considered crucial for deformation events in the Pakistani Makran and along the Murray Ridge. For the Iranian side, we envisage two scenari:

1. The Jaz Murian/Makran boundary suddenly became a backstop in Middle Miocene times, hence blocking smooth subduction and forcing wedge deformation;
2. A change from a retreating accretionary wedge to an advancing one after conjectural slab break-off or any other change of slab orientation and/or behaviour.

Uplift Processes

Surface uplift was general and does not fit the seaward picture produced by progressive accretion at the base of the wedge. A major surface uplift event occurred in Plio–Pleistocene times as indicated by the flat-lying, shallow shelf and continental sediments in Coastal Makran. Raised marine terraces along the coast and seaward migration of the coast line through historical times (e.g. Reyss et al. 1999) further demonstrates ongoing surface uplift. This observation may be a hint at the fact that tectonic underplating, i.e. blind thrusting and imbrication along and above the active décollement surface, pushes up and so strongly controls the topography behaviour. The marked relief limiting the coastal plain, to the north, may be linked to fault-propagation folding at the front of the exposed MAW system, possibly where one of the main, deforming or reactivated décollements steps downward toward the active one (Fig. 12.19).

Normal Faulting

Normal faulting in an accretionary wedge is generally attributed to the response to overthickening caused by

underthrusting (e.g. Platt 1986). This hypothesis would imply that normal faulting be widely distributed over the thick and eroded parts of the accretionary complex. This is not the case in the Iranian Makran where Plio–Pleistocene normal faults are restricted to the coastal region and are nearly absent further onshore. It is possible that these normal faults represent gravitational collapse of the active wedge in front of its backstop, which is the older wedge. Forward jump of deformation ahead of the olistostrome would have transformed the thick, older wedge into a nearly passive backstop (Smit et al. 2010). Hosseini-Barzi and Talbot (2003) considered collapse as downslope gravity spreading of weak saturated sediments lifted into anticlines above subcreted thrust culminations, but regional anticlines are very low-amplitude structures in Coastal Makran (Fig. 12.2b). Alternatively, and considering the lateral extent and strike of the coastal normal faults, one may question whether they are not delineating a zone of outer-arc, crestal grabens on a wedge bent/folded above the propagating front of a blind thrust (e.g. Emami et al. 2010), or above the front of the active subcretion system propagating from the hinterland trenchward. The second possibility would be less at odds with the several hundred meters throws on major normal faults identified on offshore seismic profiles (e.g. Grando and McClay 2006, Fig. 2419). If the Makran normal faults reflect larger scale flexural bending in the MAW, then the extensional region might indicate a Mid-Pliocene change in slab dip and subduction behaviour: If the slab became steeper, even by 1°, the elastic effects of the geometrical change on the plate would impel an oceanward shift of the trench-bulge region, hence extension with or without formation of a broad flexure in the frontal wedge. Ellouz-Zimmermann et al. (2007a) also inferred a rate or direction change in subduction during the Pliocene from the nearly undeformed platform along the Makran coastline in Pakistan.

Conclusions

The Iranian MAW was a progressively filled turbidite basin between the Middle Eocene and Middle Miocene times. Four main thrust sheets are separated by major thrusts. Inner and Outer Makran began to form before the catastrophic emplacement of the Tortonian olistostrome, which is overlain by sediments deposited in increasingly shallower water.

The composition of the blocks in the olistostrome indicates that the Imbricate Zone with its ophiolites were uplifted to near the surface before the mass-wasting event, probably as a consequence of tectonic movements.

Folding and coeval thrusting from Inner to Coastal Makran pertain to a continuous history; however, they were not strictly contemporaneous in terms of location and amplification rates of individual folds, yet developed altogether in Miocene to Pliocene times. We concur with previous conclusions (McCall 2002): The general south-vergence suggests, however, that folds and major thrusts form an imbricate structure due to bulk N–S shortening. Kilometre-scale growth structures likely formed at that time; they require more detailed mapping to be demonstrated. Deformation shifted the active, submarine wedge southward after emplacement of the olistostrome, and Coastal Makran evolved into a wedge-top basin with shallower water and continental sedimentation.

The dominant set of recent, sinistral faults, striking mainly SW-NE are parallel to transfer faults recognised offshore Pakistan, across the active front of the Makran (Kukowski et al. 2002). This latter point may confirm their still active role in the tectonic history of the MAW.

The juxtaposition of two wedges with different ages makes it difficult to average the surface slope and to conclude that Makran is a mature wedge that has one of the lowest taper angles, worldwide (e.g. Minshull and White 1989; Kukowski et al. 2001; Schlüter et al. 2002). Because of internal strain and syn-sedimentary tectonic processes, it is likely that the Makran maintained an equilibrium triangular cross-sectional shape to grow into a larger similar wedge for some periods of its evolution, and at different places.

References

Arthurton RS, Farah A, Ahmed W (1982) The late-cretaceous–cenozoic history of western Baluchistan Pakistan–the northern margin of the Makran subduction complex. In: Leggett JK (ed) Trench-forearc geology: sedimentation and tectonics on modern and ancient active plate margins, vol 10. Geological Society, London, pp 373–385

Bayer R, Chery J, Tatar M, Vernant P, Abbassi M, Masson F, Nilforoushan F, Doerflinger E, Regard V, Bellier O (2006) Active deformation in Zagros-Makran transition zone inferred from GPS measurements. Geophys J Int 165(1):373–381

Berberian F, Muir ID, Pankhurst RJ, Berberian M (1982) Late Cretaceous and early miocene andean-type plutonic activity in northern makran and central Iran. J Geol Soc London 139(5):605–614

Bernstein-Taylor BL, Brown KM, Silver EA, Kirchoff-Stein KS (1992) Basement slivers within the New Britain accretionary wedge: implications for the emplacement of some ophiolitic slivers. Tectonics 11(4):753–765

Bijwaard H, Spakman W, Engdahl ER (1998) Closing the gap between regional and global travel time tomography. J Geophys Res 103(B12): 30,055–30,078

Burg J-P, Bernoulli D, Smit J, Dolati A, Bahroudi A (2008) A giant catastrophic mud-and-debris flow in the Miocene Makran. Terra Nova 20(3):188–193

Byrne DE, Sykes LR, Davis DM (1992) Great thrust earthquakes and aseismic slip along the plate boundary of the Makran subduction zone. J Geophys Res 97(B1): 449–478

Carter A, Najman Y, Bahroudi A, Bown P, Garzanti E, Lawrence RD (2010) Locating earliest records of orogenesis in western Himalaya: evidence from Paleogene sediments in the Iranian Makran region and Pakistan Katawaz basin. Geology 38(9):807–810

Chapple WM (1978) Mechanics of thin-skinned fold-and-thrust belts. Geol Soc Am Bull 89(8):1189–1198

Critelli S, Rosa RD, Platt JP (1990) Sandstone detrital modes in the Makran accretionary wedge, southwest Pakistan: implications for tectonic setting and long-distance turbidite transportation. Sediment Geol 68: 241–260

Davis D, Suppe J, Dahlen FA (1983) Mechanics of fold-and-thrust belts and accretionary wedges. J Geophys Res 88(B2): 1153–1172

De Jong KA (1982) Tectonics of the Persian Gulf, Gulf of Oman, and southern Pakistan region. In: Nairn AEM, Stehli FG (eds) The Indian Ocean, vol 6. Plenum Press, New York, pp 315–351

Dercourt J, Ricou L-E, Vrielynck B (1993) Atlas Tethys palaeoenvironmental maps. Gauthier-Villars, Paris, p 307, 314 maps, 301plate

Desmons J, Beccaluva L (1983) Mid-ocean ridge and island-arc affinities in ophiolites from Iran: palaeographic implications. Chem Geol 39(1–2):39–63

Dolati A (2010) Stratigraphy, structure geology and low-temperature thermochronology across the Makran accretionary wedge in Iran. PhD thesis, ETH Zurich

Ellouz-Zimmermann N, Deville E, Müller C, Lallemant S, Subhani AB, Tabreez AR (2007a) Impact of sedimentation on convergent margin tectonics: example of the Makran Accretionary Prism (Pakistan). In: Lacombe O , Lavé J, Roure F, Vergès J (eds) Thrust belts and foreland basins: from fold kinematics to hydrocarbon systems. Springer, Berlin, pp 325–348

Ellouz-Zimmermann N et al. (2007b) Offshore frontal part of the Makran Accretionary Prism (Pakistan): the Chamak survey. In: Lacombe O, Lavé J, Roure F, Vergès J (eds) Thrust belts and foreland basins: from fold kinematics to hydrocarbon systems. Springer, Berlin, pp 349–364

Emami H, Vergés J, Nalpas T, Gillespie P, Sharp v, Karpuz R, Blanc EP, Goodarzi MGH (2010) Structure of the mountain front flexure along the Anaran anticline in the Pusht-e Kuh Arc (NW Zagros, Iran): insights from sand box models. In: Leturmy P, Robin C (eds) Tectonic and stratigraphic evolution of zagros and makran during the mesozoic–cenozoic, vol 330. Geological Society, London, pp 155–178

Farhoudi G, Karig DE (1977) Makran of Iran and Pakistan as an active arc system. Geology 5(11):664–668

Fruehn J, White RS, Minshull TA (1997) Internal deformation and compaction of the Makran accretionary wedge. Terra Nova 9: 101–104

Fruehn J, Reston T, von Huene R, Bialas J (2002) Structure of the Mediterranean Ridge accretionary complex from seismic velocity information. Mar Geol 186(1–2):43–58

Gansser A (1955) New aspects of the geology in central Iran. paper presented at 4th World Petroleum Congress, Roma, pp 279–300

Gansser A (1959) Ausseralpine ophiolithprobleme. Eclogae Geol Helv 52(2):659–680

Grando G, McClay K (2006) Morphotectonics domains and structural styles in the Makran accretionary prism, offshore Iran. Sed Geol 196(1–4):157–179

Hafkenscheid E, Wortel MJR, Spakman W (2006) Subduction history of the Tethyan region derived from seismic tomography and tectonic reconstructions. J Geophys Res 111: B08401, doi: 10.1029/2005JB003791

Harms JC, Cappel HN, Francis DC (1984) The Makran coast of Pakistan: its stratigraphy and hydrocarbon potential. In: Haq BU, Milliman JD (ed) Marine geology and oceanography of Arabian Sea and coastal Pakistan, Van Nostrand Reinhold Co., New York, pp 3–27

Hosseini-Barzi M, Talbot CJ (2003) A tectonic pulse in the Makran accretionary prism recorded in Iranian coastal sediments. J Geol Soc London 160(6):903–910

Jamison WR (1987) Geometric analysis of fold development in overthrust terranes. J Struct Geol 9(2):207–219

Konstantinovskaya E, Malavieille J (2011) Thrust wedges with décollement levels and syntectonic erosion: a view from analog models. Tectonophysics 502(3–4):336–350

Kopp C, Fruehn J, Flueh ER, Reichert C, Kukowski N, Bialas J, Klaeschen D (2000) Structure of the Makran subduction zone from wide-angle and reflection seismic data. Tectonophysics 329(1–4): 171–191

Kukkonen IT, Clauser C (1994) Simulation of heat transfer at the Kola deep-hole site–implications for advection, heat refraction and palaeoclimatic effects. Geophys J Int 116: 409–420

Kukowski N, Lallemand SE, Malavieille J, Gutscher M-A, Reston TJ (2002) Mechanical decoupling and basal duplex formation observed in sandbox experiments with application to the Western Mediterranean Ridge accretionary complex. Mar Geol 186(1–2):29–42

Kukowski N, Schillhorn T, Huhn K, Von Rad U, Husen S, Flueh ER (2001) Morphotectonics and mechanics of the central Makran accretionary wedge off Pakistan. Mar Geol 173(1–4):1–19

Leroy S et al. (2004) From rifting to spreading in the eastern Gulf of Aden: a geophysical survey of a young oceanic basin from margin to margin. Terra Nova 16(4): 185–192

Maruyama S, Liou JG, Tarabayashi M (1996) Blueschists and eclogites of the world and their exhumation. Int Geol Rev 38(6): 485–591

Masson F, Anvari M, Djamour Y, Walpersdorf A, Tavakoli F, Daignières M, Nankali H, Van Gorp S (2007) Large-scale velocity field and strain tensor in Iran inferred from GPS measurements: new insight for the present-day deformation pattern within NE Iran. Geophys J Int 170: 436–440

McCall GJH (1983) Mélanges of the Makran, southeastern Iran. In: McCall GJH (ed) Ophiolitic and related mélanges. Hutchinson Ross Publishing Company, Stroudsburg, Pennsylvania. Benchmark Papers in Geology/66, pp 292–299

McCall GJH (1985) Area report. East Iran Project–Area No. 1Rep., Geological Survey of Iran, Tehran, Iran, p 634

McCall GJH (1997) The geotectonic history of the Makran and adjacent areas of southern Iran. J Asian Earth Sci 15(6):517–531

McCall GJH (2002) A summary of the geology of the Iranian Makran. In: Clift PD, Kroon FD, Gaedecke C, Craig J (ed) The tectonic and climatic evolution of the Arabian Sea Region, Geological Society, London, vol 195. Special Publication, pp 147–204

McCall GJH, Kidd RGW (1982) The Makran southeastern Iran: the anatomy of a convergent margin active from Cretaceous to present. In: Leggett JK (ed) Trench-forearc geology: sedimentation and tectonics of modern and ancient plate margins vol 10. Geological Society, Special Publication, London, pp 387–397

McCall J, Rosen B, Darrell J (1994) Carbonate deposition in accretionary prism settings; early Miocene coral limestones and corals of the Makran Mountain range in Southern Iran. Facies 31(1):141–178

McQuarrie N, Stock JM, Verdel C, Wernicke BP (2003) Cenozoic evolution of Neotethys and implications for the causes of plate motions. Geophys Res Lett 30:2036. doi:10.1029/2003GL017992

Minshull TA, White R (1989) Sediment compaction and fluid migration in the Makran accretionary prism. J Geophys Res B Solid Earth Planets 94(B6): 7387–7402

Platt JP (1986) Dynamics of orogenic wedges and the uplift of high-pressure metamorphic rocks. Geol Soc Am Bull 97: 1037–1053

Platt JP, Leggett JK, Alam S (1988) Slip vectors and fault mechanics in the Makran accretionary wedge, SW Pakistan. J Geophys Res 93(B7): 7955–7973

Platt JP, Leggett JK, Young J, Raza H, Alam S (1985) Large-scale sediment underplating in the Makran accretionary prism. Geology 13: 507–511

Qayyum M, Niem AR, Lawrence RD (1996) Newly discovered Paleogene deltaic sequence in the Katawaz basin Pakistan and its tectonic implications. Geology 24(9):835–838

Ramsay JG, Huber MI (1987) The techniques of modern structural geology–vol 2: Folds and fractures. Academic, London 700

Reyss JL, Pirazzoli PA, Haghipour A, Hatté C, Fontugne M (1999) Quaternary marine terraces and tectonic uplift rates on the south coast of Iran. In: Stewart IS, Vita-Finzi C (ed) Coastal tectonics, vol 146. Geological Society, London, pp 225–237

Ricou L-E (1994) Tethys reconstructed: plates, continental fragments and their boundaries since 260 Ma from Central America to South-eastern Asia. Geodin Acta 7(4):169–218

Schlüter HU, Prexl A, Gaedicke C, Roeser H, Reichert C, Meyer H, von Daniels C (2002) The Makran accretionary wedge: sediment thicknesses and ages and the origin of mud volcanoes. Mar Geol 185(3–4):219–232

Schott B, Koyi HA (2001) Estimating basal friction in accretionary wedges from the geometry and spacing of frontal faults. Earth Planet Sci Lett 194(1–2):221–227

Şengör AMC, Altiner D, Cin A, Ustaomer T, Hsü K (1988) Origin and assembly of the Tethyside orogenic collage at the expense of Gondwana Land, vol 37. Geological Society, London, Special Publication, pp 119–181

Sepehr M, Cosgrove J, Moieni M (2006) The impact of cover rock rheology on the style of folding in the Zagros fold-thrust belt. Tectonophysics 427(1–4):265–281

Smit J, Burg J-P, Dolati A, Sokoutis D (2010) Effects of mass waste events on thrust wedges: analogue experiments and application to the Makran accretionary wedge. Tectonics 29: TC3003

Vernant P et al (2004) Present-day crustal deformation and plate kinematics in the Middle East constrained by GPS measurements in Iran and northern Oman. Geophys J Int 157(1):381–398

Vigny C, Huchon P, Ruegg J, Khanbari K, Asfaw LM (2006) Confirmation of Arabia plate slow motion by new GPS data in Yemen. J Geophys Res 111: B02402, doi:10.1029/2004JB003229

Westbrook GK, Ladd JW, Buhl P, Bangs N, Tiley GJ (1988) Cross section of an accretionary wedge: Barbados Ridge complex. Geology 16(7):631–635

White RS (1982) Deformation of the Makran accretionary sediment prism in the Gulf of Oman (North-West Indian Ocean). In: Leggett JK (ed) Trench-Forearc geology; sedimentation and tectonics on modern and ancient active plate margins, vol 10, conference. Geological Society of London, London, United Kingdom, pp 357–372

White RS, Klitgord K (1976) Sediment deformation and plate tectonics in the Gulf of Oman. Earth Planet Sci Lett 32(2):199–209